Meas. Sci. Technol. 6 (1995) 1582–1587. Printed in the UK

An optical instrument for monitoring the internal conditions of high-voltage circuit breakers

E Colombo†, E Emolumento‡, M Menchise§, E Paganini§, V Piemontese§, L Placentino‖ and G Tondello‖

† ENEL, Centro Ricerche Elettriche, Cologno Monzese, Milano, Italy
‡ CESI, Milano, Italy
§ CISE, Segrate, Milano, Italy
‖ Università di Padova, Dipartimento di Elettronica ed Informatica, Padova, Italy

Received 29 December 1994, in final form 26 June 1995, accepted for publication 12 July 1995

Abstract. A new optical instrument is described which images the arc discharges which originate inside SF_6 gas high-voltage circuit breakers at the moment of contact separation, while it follows the time evolution. The instrument performs a series of double simultaneous discharge images, with adjustable exposure times between 7 and 80 μs and frame rate $\leq$ 2 kHz. The instrument design principles, realization details and characterization measurements are reported and discussed. Finally, the first measurements carried out by the instrument on a real breaker are reported.

1. Introduction

The study of arc discharges which appear inside SF_6 high-voltage breakers is important both for a better phenomenon understanding and for application purposes. It is desirable to obtain diagnostics on the breaker itself and, more specifically, on the arcing contacts in order to optimize them during the design and exercise phases.

One of the most powerful monitoring tools is the spectroscopic analysis of radiation emitted by the elements excited and ionized during the arc discharge. The emitting elements can originate from the gas (S, F) or from the contacts (Cu and W typically) [1].

Previously another innovative instrument was designed and realized which allowed one to observe and record transient phenomena in the visible range with simultaneous spectral, spatial and time resolution [2]. By means of this instrument a series of experimental observations of the arc discharges inside SF_6 breakers was carried out. A remarkable part of the experimental work consisted of the observation and recording, within the visible range, of the Cu characteristic emissions coming from the contacts. The most interesting Cu lines were observed to be at 4509 and 5292 Å. In fact, other even stronger lines were observed, but they all appeared to be 'polluted' by spectrally near lines coming from other elements (typically S and F).

A remarkably interesting observed phenomenon was the presence of 'jets', that is localized Cu emissions which do not spatially coincide with the main discharge. Unfortunately the instrument allowed spatial resolution along only one direction; it was therefore impossible to determine the spatial structure of the jets.

In order to continue with research into Cu emissions the new instrument, which allows visualization of their spatial distribution, was designed and realized. This instrument performs two bidimensional images of the discharge region near the breaker fixed contact at two different wavelengths; these images of the same spatial region are carried out at the same time. Therefore, by properly selecting the wavelengths, it is possible to distinguish the main discharge emissions from the Cu emissions; it is also possible, when processing the data, to subtract the continuum from the Cu emissions in order to evaluate the latter quantitatively.

The phenomenon of Cu emission is strongly variable from shot to shot; moreover, for any interruption, it evolves with times of the order of the current oscillation period. As a consequence it is necessary to perform measurements on every current interruption and follow the time evolution of the emissions during times variable between 5 and 15 ms, according to the length of light emission. This condition imposed the use of a purposely developed imaging system. It is composed of two CCD fast cameras and the related acquisition units and allows the recording of images with a 2 kHz frame rate. From measurements carried out in the past with the help of high-speed frame cameras the arc is known to show spatial instabilities with times of the order of microseconds. Therefore the single frame exposure time has to be comparable with such times, in order to avoid spatial smearing of the image. For this reason the new instrument is equipped with a shutter which allows adjustment of the exposure time within the range 7–80 μs.

0957-0233/95/111582+06$19.50

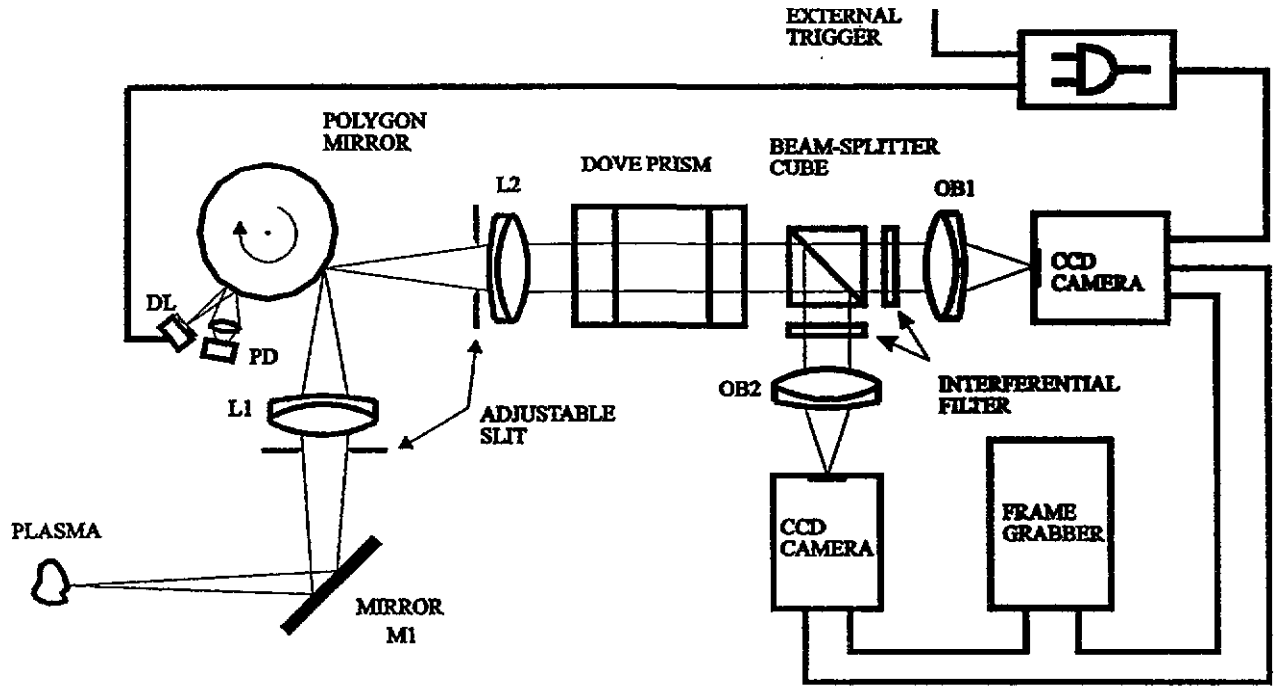

Figure 1. Instrument layout.

Table 1. Values of the most meaningful system parameters.

Parameter	Operating value	Measurement unit
L1 focal length	130	mm
L1 magnification	1/10.4	
L2 focal length	160	mm
Rotating mirror frequency[a]	67	Hz
First slit width[b]	1	mm
Second slit width[b]	1	mm
OB1, OB2 focal length	50	mm
OB1/L2 magnification	1/3.2	
OB2/L2 magnification	1/3.2	
Total magnification	1/33.3	
Filter centre wavelength	5292 5275 5321	Å
Filter bandwidth	10	Å
Exposure time[c]	12	μs
Image dimensions	128 × 64 (2 × 1)	pixel (mm)
Frame rate	1.7	kHz
Maximum number of storable frames	30	

[a] Selectable value within the range $20 \div 220$ Hz.

[b] Selectable value within the range $0 \div 3$ mm.

[c] Selectable value within the range $7 \div 80$ μs.

In the following the design, realization and characterization of the new instrument are described. Some results obtained during the first measurements 'in field' are reported and discussed in section 4.

2. Instrument description

The instrument has to perform a series of double images of the discharge, at two selectable wavelengths, with a short exposure time (≈ 15 μs) and frame rates up to 2 kHz.

The selection of the wavelengths is made by two interferential filters. Both the centre wavelength and the bandwidth can therefore be chosen within the visible range. Actually the measurements were carried out by filters with centre wavelengths corresponding to Cu and S emission lines and to the adjacent continuum.

The exposure times of approximately 10 μs are imposed by the arc instability characteristic times. It is necessary to use a fast shutter in order to obtain these. The use of ferroelectric devices and of gated image intensifiers

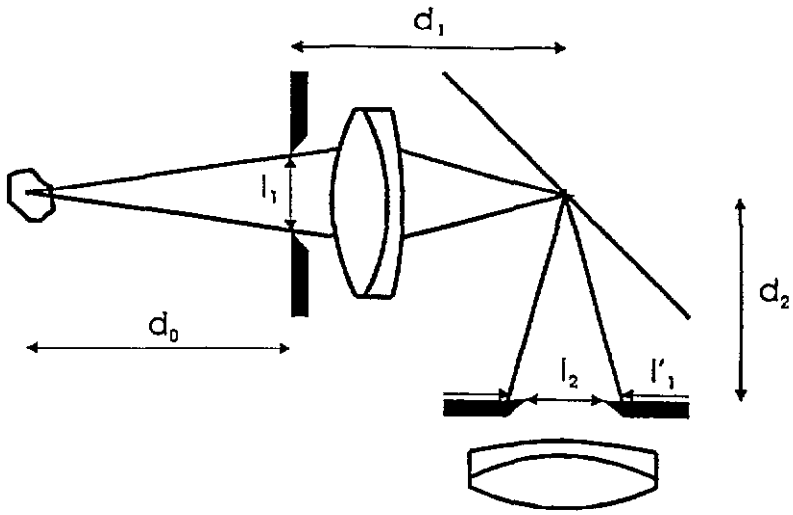

Figure 2. Shutter layout.

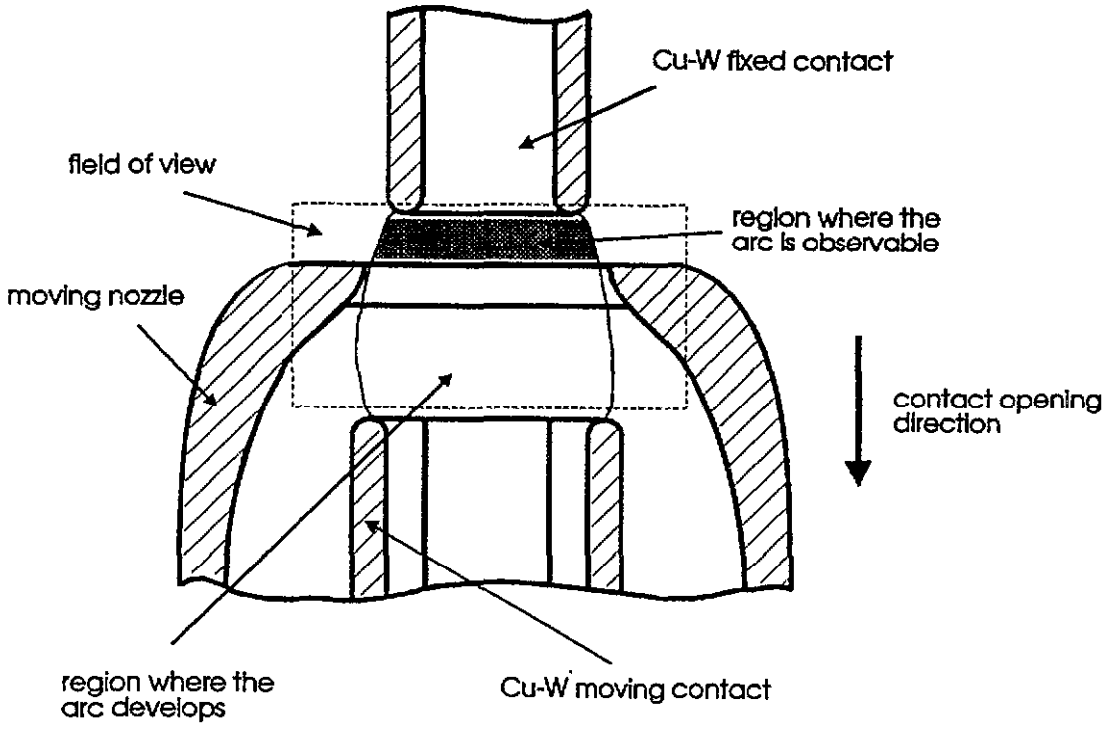

Figure 3. Schematic view of the contact region.

was taken into account. The first ones were discarded as they are too slow (minimum shuttering time $\approx$ 100 μs). The image intensifiers, even if very fast, show an output brightness which is too low for fast cameras with high frame rates. Thus the shutter function was carried out by a 24 facets rotating mirror.

The 2 kHz frame rate imposed the use of fast cameras with a related acquisition system which had been already developed for the previous instrument [2, 3], while the optical system was purposely designed and realized for this application.

The instrument layout is shown in figure 1. The numerical values of the most meaningful parameters which were used during the preliminary measurements are reported in table 1.

The lens L1 forms an image of the arc discharge onto a rotating mirror facet; the image is so demagnified as to be contained within a rotating polygon facet and to avoid vignetting effects. By adjusting the mirror M1 it is possible to select the observed part of the arc.

The light is diverted by the mirror, then gathered by the lens L2 and sent to a Dove prism which allows image rotation around the optical axis. This allows the images to be properly oriented onto the CCDs. A beamsplitter cube at the prism output shares the main beam into two parts; the two derived beams are sent through two interferential filters. Finally a properly reduced image is formed onto the CCDs by the photographic objectives OB1 and OB2. A two lens system was selected with the lens L2 set at the focal distance from the rotating mirror and the objectives OB1 and OB2 set at the focal distance from the CCDs in order to minimize the divergence of the beam incident

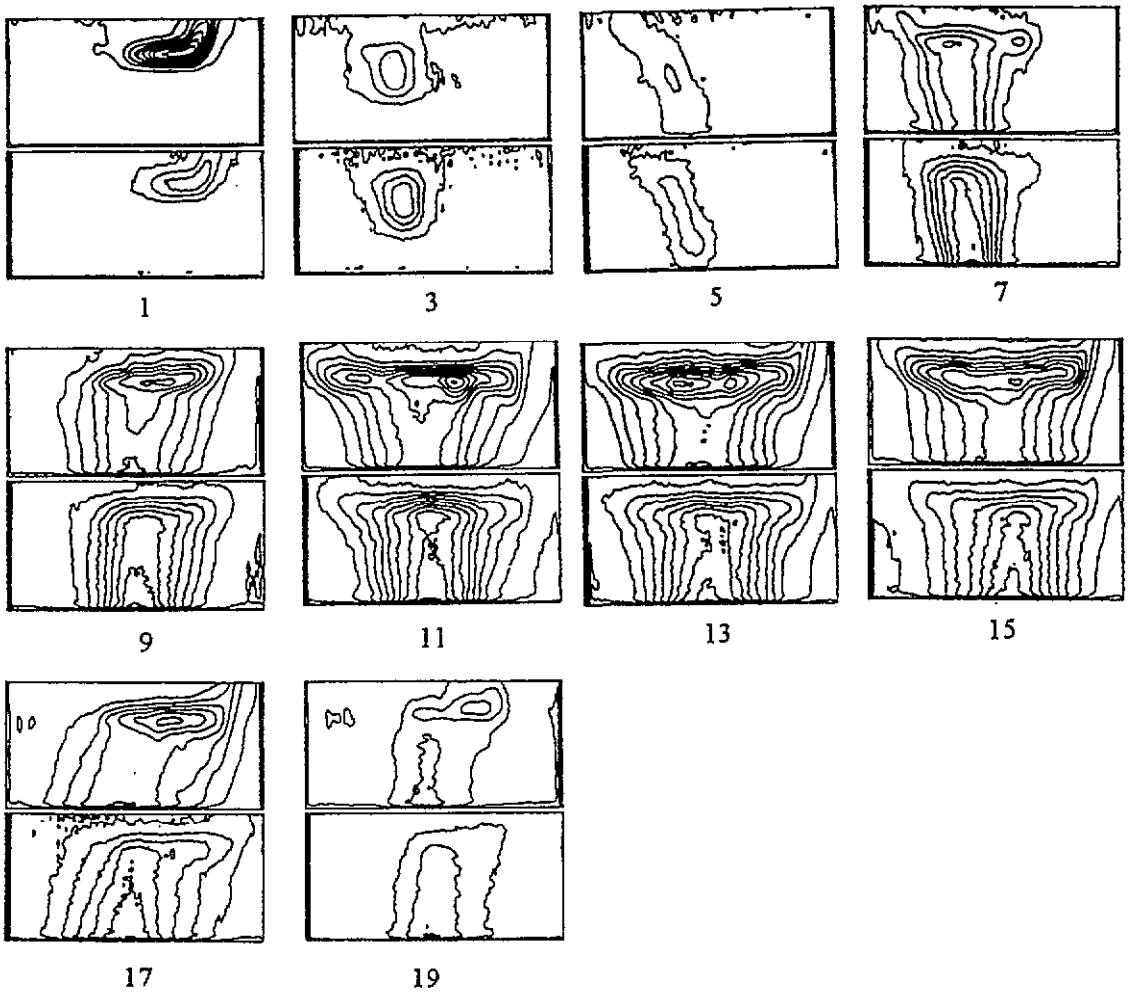

Figure 4. Time evolution of the arc emissions. Double discharge images, recorded at the same time, are displayed. For the sake of clarity only half recorded frame pairs (odd numbers) are shown. Upper frame with filter centred at 5292 Å (CuI emission); lower frame centred at 5321 Å (SII emission). Time separation between successive displayed frame pairs is 1240 μs. Field of view: 66 mm horizontal; 33 mm vertical.

onto the filters (in fact the filter centre wavelength changes as the incidence angle changes). In this way a maximum divergence of 1.3°, due to the extension of the source image on the mirror, was reached. This implies a filter centre wavelength shift of 0.1 nm, which turns out to be lower than the bandwidth of the used filters (1 nm).

The two slits and the rotating mirror carry out the function of time shutter. The light coming from the first slit scans along the second slit by means of the rotating mirror. As a consequence there is light onto the detectors during all the time the beam needs to scan along the second slit.

The detection system is made up of two cameras [3] which are able to record simultaneously the two images of the same arc portion at two different wavelengths. It is important that the two images are recorded at the same time and spatially coincide pixel by pixel because during subsequent image processing it can be important to subtract the two frames relatively. Successive images correspond to successive mirror facets; then the image acquisition has to be synchronized both with the external event, namely the arc discharge, and with the instant the light enters the second slit. For this purpose a trigger signal is generated by the photodiode (PD) which detects light emitted by the laser diode (DL) and reflected by the rotating mirror. Then a logical AND gate between this trigger and a signal synchronized with the external event is produced. The output signal is used to start the image acquisition of the cameras, which turns out to be synchronous because the clock signal is common.

The outputs of the cameras are digitized by a proper acquisition unit which allows storage of up to 30 frames per channel. Finally dedicated software allows a first processing of the images and their visualization. A detailed description of the cameras and their acquisition systems has already been reported [2, 3].

3. Instrument characterization

The basic parameters for the instrument are T, the exposure time, and E, the energy gathered by the CCDs during a single frame. The system selected to carry out the shutter function requires a trade off between the two opposite constraints to have short exposure times and enough light on the detectors. As both these parameters depend on the widths of the two slits, it is necessary to establish the conditions for the maximization of the gathered energy, once the measurement exposure time is selected.

With reference to the figure 2, define T as the overall time of light presence on the second slit. If a point source is taken into account, it follows:

$$T = \frac{l_1 d_2 + l_2 d_1}{4\pi f d_1 d_2} \qquad (1)$$

where l_1 is the first slit width, l_2 is the second slit width, f is the rotating mirror frequency, d_1 the distance between the first slit and the mirror and d_2 the distance between the mirror and the second slit. I is the intensity on the second slit plane and h the height, which is the same for both the slits. The total gathered energy can then be written as:

$$E = \frac{Ih}{4\pi f d_1}(4\pi f d_1 T l_2 - l_2^2). \qquad (2)$$

Once the exposure time for the measurements is selected, there are many slit pairs which satisfy the following condition, but only one which maximizes the total gathered energy, and precisely the pair which satisfies the condition $l_2 = l_1 d_2/d_1$.

A series of characterization measurements was carried out by setting a point source in the object plane of the optical system. The point source was realized by focusing the light coming from a laser onto a scatterer. Therefore the system instrumental function was established; it turned out to show a near Gaussian shape with a FWHM $\approx$ 3 pixels. Moreover a set of measurements was carried out in order to verify equations (1) and (2). These measurements showed that, by checking the slit dimensions with an accuracy of 5%, it is possible to know the exposure time and the gathered energy with an accuracy better than 10%. This characterization allows one to select the operating conditions for the 'in field' measurements, by properly selecting the dimensions of the two slits.

4. Preliminary measurements and first results

A first set of measurements on a real device was carried out in order to verify the operating capability of the instrument. The working conditions of the optical instrument are reported in table 1. A series of measurements was carried out on a SF_6 breaker with a pair of new contacts, with a 30 kA effective current value at 50 Hz and a 17 ms arcing time.

The device under test is a pole of dead tank puffer-type circuit breaker equipped with two glass windows; it has 0.8 m^3 volume and 170 kV nominal voltage. Actually the tests were carried out at a 17 kV voltage; this required a re-ignition circuit to increase the arcing time. The arcing contacts are made of sintered Cu 30%–W 70%. During the switching-off operation, mechanical separation of the contacts induces production of the arc which is axially blown by cold gas. The gas flux along the contact axis is controlled by a Teflon nozzle which is integral to and concentric with the moving contact.

Figure 3 shows a section of the contact system approximately 7 ms after the contact opening. The instrument field of view is of 66 × 33 mm^2 and is indicated in the figure by the broken line. The moving contact (down)

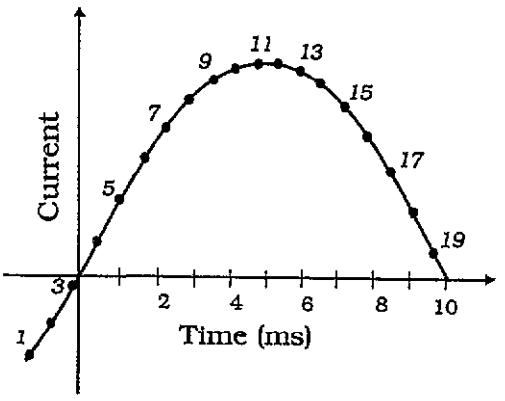

Figure 5. Time correspondence between the numbers of recorded frame pairs and the instantaneous current.

is mechanically opened and moves at a rate of 6 m s^{-1}. In order to achieve a longer view of the arc developement, the nozzle was cut so as to make the arc visible after only 6 ms the separation of the contacts. Since the overall arc time is 17 ms, the useful observation time is 11 ms, corresponding to 19 frames.

Figure 4 shows the results related to a test performed when the contacts had already cumulated a total broken current of 300 kA. The images are to be read as follows. There are ten recorded frame pairs following one another every 1240 μs; as a matter of fact in the original display there were 22 frame pairs every 620 μs. The intensity is pictured by iso-level curves (pseudo colours in the original display); the intensity increases towards the interior. The upper frame refers to a filter centred at 5292 Å, corresponding to the emission wavelength of a CuI line; the lower frame refers to a filter centred at 5321 Å, corresponding to the emission wavelength of a SII line. The time correspondence between the frame pairs and the instantaneous current is shown in figure 5.

The SII line was chosen for two reasons. The first is that the continuum intensity is proportional to the SII intensity, except for small differences depending on the temperature, and consequently the two lines show the same spatial behaviour. In fact the ion SII is the only ion present, hence the electronic density n_e is equal to the SII density n_{SII}. In the case where the upper level of the SII emission line is populated predominantly by recombination processes, the line intensity is proportional to $n_{SII} n_e = n_e^2$; on the other hand the intensity of the emitted continuum, mainly produced by collision processes, is also proportional to n_e^2. Therefore the SII intensity, multiplied by a proper coefficient, is representative of the continuum and can be used in the data processing in order to evaluate quantitatively the Cu line intensity by difference. The second reason is the possibility of comparing the spatial distribution of Cu and of the main discharge, which coincides well with the SII emissions.

With reference to figure 4, in the frame pair number 1 the arc has already appeared and appears more and more vertically extended as the Teflon nozzle moves down, ultimately occupying the whole field of view from pair number 7 onwards. The emission intensity maximum is

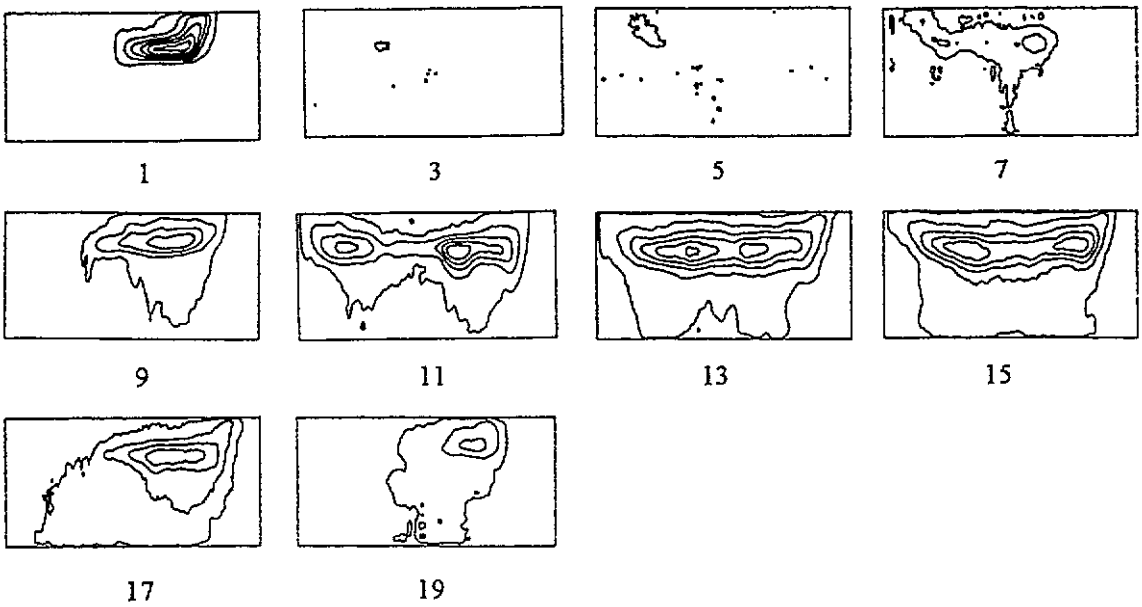

Figure 6. Time evolution of CU emissions as subtracted from the continuum emissions. Time separation between two successive frames is 1240 μs.

reached in pair 13, just after the current peak. More generally, from the observation of other tests, the maximum intensity is seen to experience some delay with respect to the current peak. The second current zero coincides with arc extinction and corresponds approximately to pair number 20 (not shown in figure 4). In the upper part of some frames the fixed contact is clearly visible.

The lower frames, related to SII emissions and representative of the main discharge, show typical arc behaviour—that is spatially unstable at low instantaneous currents and more stable when corresponding to the higher currents.

The most interesting result is given by the difference between Cu and S emissions. In fact, while the S emissions, which represent the main discharge well, are in any case at the centre of the frame and are equally intense along the vertical direction, the CuI emissions (upper frames) show quite a different behaviour. They are only present near the fixed contact and quickly decrease at a vertical distance of 10 mm from it. On the other hand Cu emissions appear to be horizontally wider, corresponding to the whole width of the fixed contact.

The final result of the first data processing on the images shown in figure 4 is reported in figure 6 and displays the spatial position and time evolution of Cu emissions. Figure 6 was obtained by subtracting, from the image related to Cu emission, the contribution of the continuum evaluated by multiplying the SII intensity by a proper coefficient. In short, with reference to figure 4, the lower frames were subtracted pixel by pixel from the upper frames. It is worth noticing that, since the emission of the continuum is related to the electron presence, in the spatial region out of the main discharge the continuum contribution to be subtracted is very small and the non depurated Cu emission (figure 4, upper frames) practically coincides with the depurated one (figure 6). In figure 6 the whole history of Cu emissions without continuum contribution during the test at 300 kA total broken current can be followed. In frame 1 the Cu radiates near the electrode and partly follows its outline. In the first frames the arc image is cut off by the lowering moving contact. In frame number 3 there is practically no emission: it corresponds to the first current zero. Finally the frames of the second half-period are displayed as far as the second current zero, corresponding to frame 20 (not shown in the figure); the emission intensity follows the instantaneous value of the current, with low intensity next to the current zero and high intensity just after the current peak. In all frames the Cu emission is spatially located near the contact. These preliminary results show the Cu emission to be clear and easily measurable.

5. Conclusions

The design, characterization and first successful use of an innovative instrument have been described. The instrument can be used to monitor the state of high-voltage breaker contacts. Further investigations into this subject are in progress.

References

[1] Okuda S, Ueda Y, Murai Y, Miyamoto T, Doi Y and Venosono C 1980 Spectroscopic approach to the analysis of high current arcs in SF_6 *IEEE Trans. Plasma Sci.* **8** 395–9

[2] Bargigia A, Emolumento E, Liguori C, Paganini E, Piemontese V and Tondello G 1992 A spectroscopic system using fast CCD detectors for space and time resolved diagnostics of arc discharges *J. Meas. Sci. Technol.* **3** 992–6

[3] Paganini E, Perini U, Bargigia A and Tondello G 1990 Un sensore CCD bidimensionale veloce per analisi spettroscopiche su plasmi *Atti del Convegno Elettroottica (Milano)* pp 557–60